6-DoF EKF SLAM with global planar features in artificial environments

Ryota Ozaki[1] and Yoji Kuroda[2]

Abstract— This paper presents online SLAM for self-localization of mobile robots in artificial environments. This proposed method exploits global planar features as landmarks in extended Kalman filter (EKF). The main purpose of using global planer features is reducing accumulative error of the estimation. Planes are extracted from point cloud of 3-D LiDAR as normals. These normals are projected onto "depth-Gaussian sphere". Those points from each plane are concentrated in one place on the sphere since planes has many normals which are almost same directions. These concentrations of points are deemed as planar features. The state vector of EKF has states of both a robot and landmarks. Prediction steps compute integration of angular velocity from gyroscope and linear velocity from wheel encoders, respectively. Observation steps update the states by associating observed planes and landmark planes. Area of landmark planes are also expanded with every association. Observed planes which are not associated with any landmarks become new landmarks, and the state vector is augmented. Similar landmarks are merged as necessary. To avoid mismatching between observations and landmarks, candidates for the association are selected by some conditions. To evaluate the proposed method, an experiment with an actual robot was performed. It shows the method suppresses accumulative error of self-localization by using the landmarks.

I. INTRODUCTION

Estimating the pose of a robot in the surrounding environment is one of the classic problems of mobile robotics. In a known environment, the robot can self-localize by matching sensor information at the moment to the prior information of the environment. Especially, many methods using maps as prior information have been proposed [1]. In those methods, accuracy of the map is important. However, mapping requires accurate estimation of the robot's pose. This leads a dilemma: for self-localization, the robot requires a map, but to build such a map, the pose of the robot must be known [2]. A solution of this is SLAM (Simultaneous Localization And Mapping) [3]. Many kinds of SLAM have been developed. This paper focuses on online (real-time) SLAM because localizing the pose and correcting estimation online is required when the robot runs in unknown environments. SLAM with scan matching method such like ICP scan matching [4], NDT scan matching [5], [6] is one of well-known online SLAM. Zhang [7] has proposed a matching method based on edge and planar features with good results. Using these features achieves low-drift and low-computational complexity. On the other hand, it is difficult for scan matching methods to correct accumulative error because it integrates relative pose transformation to the initial pose. On another hand, landmark-based SLAM can suppress error while the robot is observing the landmarks. Taguchi [8] has proposed a method which associates observation and landmarks, and applies SVD to estimate the pose of the robot. But using SVD means noise of observation is not considered. Landmark-based SLAM implemented with EKF is well known [9]. Exploiting planes as landmarks is a well known method in the area of visual SLAM [10], [11], [12]. However they do not describe how to handle landmarks which the robot pass by and can not be observed. It means it is not considered how to deal with the situation that robot comes back to known place, and how to avoid false matching. Some methods use planar landmarks with Manhattan world assumption [13], [14]. The assumption assumes that planes in the environment are orthogonal to each other. This assumption has low versatility although it linearizes the system and makes estimation easier.

To address these issues above, this paper proposes EKF SLAM with global planar features as landmarks. And data association including the situation that the robot comes back to known landmarks is implemented. Note that the proposed method does not use any prepared maps nor models of the environment. Information of the planar landmarks such like position and orientation are also unknown. And Manhattan world assumption is not used in this method, which means any planes can be used in this method.

Main contributions of this paper are summarized here:

- A method of extracting planes from point cloud as normals is described.
- EKF framework with planar landmarks is described.
- Data association between sensor observations and landmarks including the revisit situation is described.
- Condition setting for avoiding false matching is described.

II. 6-DoF EKF SLAM WITH GLOBAL PLANAR FEATURES IN ARTIFICIAL ENVIRONMENTS

The system configuration diagram of the proposed method is shown in Fig. 1. The method is based on landmark-based SLAM [3]. Prediction step and update step are repeated in EKF. Date association between observations and registered landmarks is needed for the update process. Landmarks means planar features in this method. The planar features are extracted from the point cloud.

A. Extraction of planes from point cloud

1) Generation of normal-cloud: Normal-cloud **N** is generated by applying principal component analysis (PCA)[15] to the local neighbor points of each query point in point

[1]Ryota Ozaki is with Graduate School of Science and Technology, Meiji University, Kanagawa, 214-8571, Japan `ce192021@meiji.ac.jp`
[2]Yoji Kuroda is with Graduate School of Science and Technology, Meiji University, Kanagawa, 214-8571, Japan `ykuroda@meiji.ac.jp`
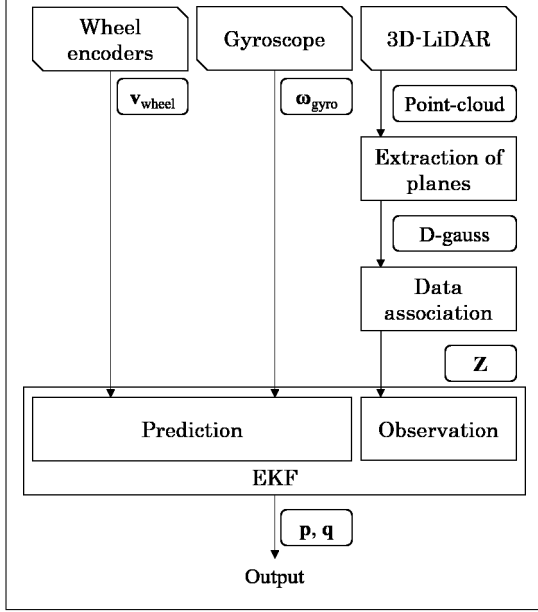
Fig. 1: System architecture

Fig. 2: Depth-Gaussian sphere

cloud that is obtained with 3-D LiDAR. The neighbor points (query point cloud) $\mathbf{C}_{\text{query}}$ are searched by kd-tree[16] with searching radius. This searching radius is set larger at farther point since point density is more sparse in farther area.

$$\mathbf{C}_{\text{query}} = \begin{bmatrix} \mathbf{c}_0 & \cdots & \mathbf{c}_{n_{\mathbf{C}\text{query}}} \end{bmatrix}, \quad \mathbf{c}_i = \begin{pmatrix} c_{i,x} & c_{i,y} & c_{i,z} \end{pmatrix} \quad (1)$$

$$\mathbf{N} = \begin{bmatrix} \mathbf{n}_0 & \cdots & \mathbf{n}_{n_{\mathbf{N}}} \end{bmatrix}, \quad \mathbf{n}_i = \begin{pmatrix} n_{i,a} & n_{i,b} & n_{i,c} & n_{i,d} \end{pmatrix} \quad (2)$$

where $\mathbf{c}_i$ denotes a point, and $\mathbf{n}_i$ denotes parameters of the plane (i.e. $n_{i,a}x + n_{i,b}y + n_{i,c}z + n_{i,d} = 0$).

2) Selection from normal-cloud: Query point clouds which have high flatness are picked up from the normal-cloud with their third eigenvector (normal) by the conditions below.

- The number of query points $n_{\mathbf{C}\text{query}}$ is large enough.

$$n_{\mathbf{C}\text{query}} > \text{TH}_{n_{\mathbf{C}\text{query}}} \quad (3)$$

- Fitting error between the plane and neighbor points e is small enough.

$$e = \sum_{i=0}^{n} \frac{|n_a c_{i,x} + n_b c_{i,y} + n_c c_{i,x} + n_d|}{\|\mathbf{n}\|} < \text{TH}_e \quad (4)$$

3) Generation of depth-Gaussian sphere: All initial points of selected normals $\hat{\mathbf{N}}$ ($\in \mathbf{N}$) are moved to one origin and generate point cloud $\mathbf{C}_{\text{d−gauss}}$. Shimizu [17] calls this point cloud "depth-Gaussian sphere" (cf. Gaussian sphere [18]). Fig. 2 shows an outline drawing of depth-Gaussian sphere.

$$\mathbf{C}_{\text{d−gauss}} = \begin{bmatrix} \mathbf{c}_{\text{d−gauss}_0} & \cdots & \mathbf{c}_{\text{d−gauss}_{n_{\hat{\mathbf{N}}}}} \end{bmatrix}$$
$$\mathbf{c}_{\text{d−gauss}_i} = -n_{i,d} \begin{pmatrix} n_{i,a} & n_{i,b} & n_{i,c} \end{pmatrix} \quad (5)$$

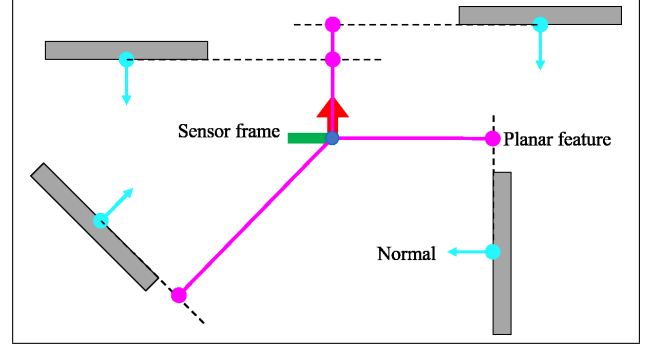*4) Clustering in depth-Gaussian sphere:* Euclidean clustering is applied to the point cloud on depth-Gaussian sphere. And clusters which has enough many numbers of members are extracted as plane. Centroid of each extracted cluster is used as planar feature below.

B. EKF framework

The state of both the robot and planar landmarks are estimated simultaneously in this EKF. The state vector $\mathbf{x}$ consists the state of them as Eq. (6). Prediction process is done with input of wheel encoders and gyroscope. Observation process is done with observation of planar landmarks.

$$\mathbf{x} = \begin{pmatrix} \mathbf{p}^{\text{T}} & \mathbf{q}^{\text{T}} & \mathbf{m}_0^{\text{T}} & \cdots & \mathbf{m}_n^{\text{T}} \end{pmatrix}^{\text{T}}$$
$$\mathbf{p} = \begin{pmatrix} x_{\text{r}} & y_{\text{r}} & z_{\text{r}} \end{pmatrix}^{\text{T}}, \quad \mathbf{q} = \begin{pmatrix} \phi_{\text{r}} & \theta_{\text{r}} & \psi_{\text{r}} \end{pmatrix}^{\text{T}} \quad (6)$$
$$\mathbf{m}_i = \begin{pmatrix} x_{\text{lm},i} & y_{\text{lm},i} & z_{\text{lm},i} \end{pmatrix}^{\text{T}}$$

where $\mathbf{p}$ denotes the position of the robot, $\mathbf{q}$ denotes the posture of the robot, and $\mathbf{m}_i$ denotes the position of the landmark.

1) Prediction with wheel encoder and gyroscope: Linear velocity measured with wheel encoder $\mathbf{v}_{\text{wheel}}$ and angular velocity measured with gyroscope ω_{gyro} are transformed from the local coordinate to the global coordinate.

$$\mathbf{u}_{\text{wheel}} = \mathbf{v}_{\text{wheel}} = \begin{pmatrix} v_x & 0 & 0 \end{pmatrix}^{\text{T}} \quad (7)$$

$$\mathbf{u}_{\text{gyro}} = \omega_{\text{gyro}} = \begin{pmatrix} \omega_x & \omega_y & \omega_z \end{pmatrix}^{\text{T}} \quad (8)$$

$$f\{\mathbf{x}_k\} = \mathbf{x}_k + \begin{pmatrix} \mathbf{Rot}_{xyz}^{\text{l}\rightarrow\text{g}}\{\mathbf{q}_k\}\mathbf{u}_{\text{wheel},k}\Delta t \\ \mathbf{Rot}_{\phi\theta\psi}^{\text{l}\rightarrow\text{g}}\{\mathbf{q}_k\}\mathbf{u}_{\text{gyro},k}\Delta t \\ \mathbf{0}_{3\times n} \end{pmatrix} \quad (9)$$

where $\mathbf{Rot}_{xyz}^{\text{l}\rightarrow\text{g}}$ is the rotation matrix which transforms the point from the local frame to the global one, and $\mathbf{Rot}_{\phi\theta\psi}^{\text{l}\rightarrow\text{g}}$ is the rotation matrix which transforms the angles from the local frame to the global one.

2) Observation of planar landmarks: Observation process is done when observations of planar features are associated with known landmarks. When the observations is not associated with any landmarks, the state vector is augmented and the state of the new landmark is added. How to associate

between observations and landmarks is described in next section.

$$\mathbf{Z} = \begin{pmatrix} \mathbf{z}_0^{\mathrm{T}} & \cdots & \mathbf{z}_n^{\mathrm{T}} \end{pmatrix}^{\mathrm{T}}$$
$$\mathbf{z}_i = -n_{i,d} \begin{pmatrix} n_{i,a} & n_{i,b} & n_{i,c} \end{pmatrix}^{\mathrm{T}} \tag{10}$$

$$\mathbf{Z_p} = \begin{pmatrix} \mathbf{z_{p_0}}^{\mathrm{T}} & \cdots & \mathbf{z_{p_n}}^{\mathrm{T}} \end{pmatrix}^{\mathrm{T}}$$
$$\mathbf{z_{p}}_i = h_i\{\mathbf{x}_k\} = \mathbf{Rot}_{\mathrm{xyz}}^{\mathrm{g}\to 1}\{\mathbf{q}_k\}(\mathbf{m}_{i,k} - \frac{\mathbf{p}_k \cdot \mathbf{m}_{i,k}}{\|\mathbf{m}_{i,k}\|^2}\mathbf{m}_{i,k}) \tag{11}$$

where $\mathbf{Z}$ is the observation vector, and $\mathbf{Z_p}$ is the predicted observation vector. Fig. 3 shows the function of $h_i\{\mathbf{x}\}$.
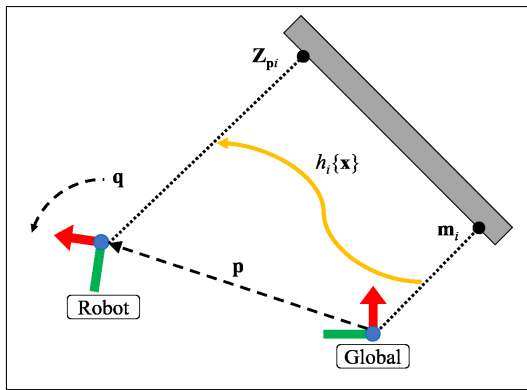

Fig. 3: Predicted observation

C. Data association

1) Search for a corresponding landmark: Each registered landmark searches observation which has minimum Mahalanobis distance $d_{\mathrm{Mahalanobis,min}}$. When the distance is smaller than the threshold, the observation is associated with the known landmark. When it is larger, the observation is registered as a new landmark.

$$d_{\mathrm{Mahalanobis,min}} = \mathbf{y}_{\hat{i}}^{\mathrm{T}}\mathbf{S}_{\hat{i}}^{-1}\mathbf{y}_{\hat{i}} < \mathrm{TH}_{d_{\mathrm{Mahalanobis}}}$$
$$\mathbf{y}_i = \mathbf{z}_i - \mathbf{z_{p}}_i, \quad \mathbf{S} = \mathbf{J_h}\mathbf{P}\mathbf{J_h}^{\mathrm{T}} + \mathbf{R} \tag{12}$$

where $\mathbf{J_h}$ is the Jacobian of the vector $\mathbf{z_p}$, $\mathbf{P}$ is the covariance matrix, and $\mathbf{R}$ is the noise matrix of observation.

2) Registration of a new landmark: A new landmark is registered and initialized with the information below:

- Own coordinate (origin)
  The point which the landmark is observed at the first time becomes its origin of the own coordinate.
- Observed range
  Each landmark records the range which the robot has observed it before in the coordinate of the landmark.
- Direction of normal
  Planes can have two direction of normal. But only one side of the planes can be observed in the real world because walls and other things have thickness. Therefore the direction of the plane is registered when the landmark is initialized.

3) Update of information of associated landmark: When observation is associated with the observation, the information of the landmark below is updated.

- Orientation of coordinate
- Observed range

4) Merge of landmarks: Landmarks are merged when two or more landmarks find a same observation as a corresponding one. The oldest landmark which is observed earliest is remained, and the others are absorbed to the oldest one. The range which the robot has observed the landmark is also merged. This merge can happen when the robot comes back to the known place.

However, landmarks are not merged when these landmarks have been observed at the same time at prior step. At that time, only the landmark whose Mahalanobis distance $d_{\mathrm{Mahalanobis,min}}$ is smaller is associated, and the others have no pair.

5) Narrowing down the candidates: In order to avoid false association, registered landmarks are narrowed down every step before association process above. Geometric constraints that the method exploits are here:

- Only one side of the plane is visible and it is not visible from the other side.
- The landmark is not visible from a far position from the last position of the robot where the landmark is observed (observed range) like Fig. 4.
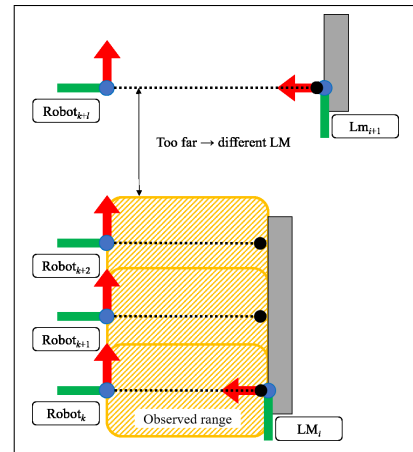

Fig. 4: Observed range

III. EXPERIMENTS

A. Experimental outline

In this experiment, the 6-DoF pose (position and attitude) of the robot was estimated by the proposed method and comparative approaches while the robot moved. It is hard to get all ground truth of the pose while the robot is moving. Hence, the robot was driven back to the exact starting position. Thus, the return position error and the return attitude error were evaluated instead of the whole trajectory.

B. Experimental conditions

1) Hardware: The experimental mobile robot is shown in Fig. 5. It has Velodyne HDL-32E，Xsens MTi30 and wheel encoders.
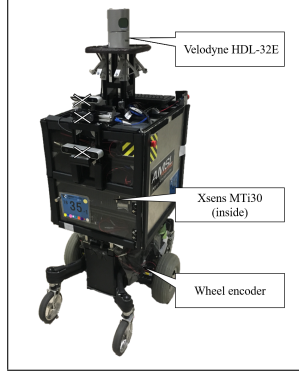

Fig. 5: The experimental robot

2) Environment: The experimental floor map is shown in Fig. 6. An planar obstacle was put in the environment in order to make sure that the proposed method does not use Manhattan world assumption. The robot was driven for three rounds of this course.
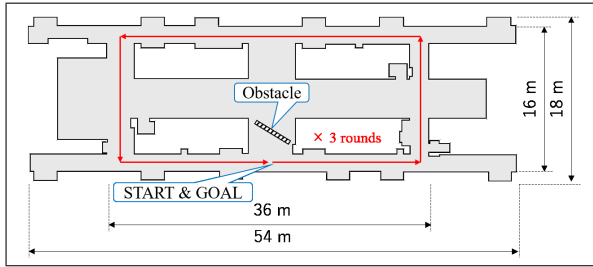


Fig. 6: The experimental floor map

3) Comparative approaches:
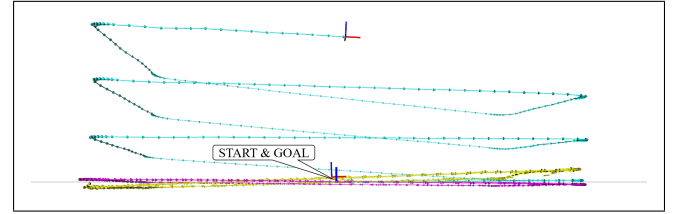- Gyrodometry [19]
- LOAM [7]

C. Experimental result

Trajectories estimated by the proposed method and the comparative approaches on x-y plane are shown in Fig. 7a. The trajectories on x-z plane are shown in Fig. 7b. The return position error and the return attitude error are shown in Table I. The proposed method estimated the pose of the robot with less error in Euclidean distance compared with the others. It was stable by using global planar features. The method could correct the estimation as long as the robot observes the registered planar landmarks. And some landmarks were merged when the robot came back to the start point from the other side. On the other hand, it was hard for gyrodometry and LOAM to correct accumulative error while it was driven. Although LOAM estimated transformation of the pose well each step, once it detected bad matching, it was hard to correct, which is comes from the feature of scan matching method. The average time consumption of the proposed

method is 0.113 sec for extraction the planar feature, and 0.009 sec for the association and updating the state vector.
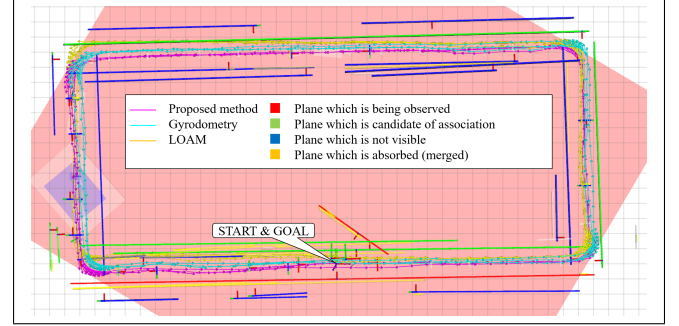
(a) x-y (with registered global planes)

(b) x-z

Fig. 7: The estimated trajectories

TABLE I: Return position error and the return attitude error

error in...	Proposed method	Gyrodometry	LOAM
x[m]	-0.042	+0.600	-0.338
y[m]	+0.019	+0.314	+0.359
z[m]	+0.004	+9.753	+0.341
d_{Euc}[m]	0.046	9.776	0.600
ϕ[deg]	+0.03	+2.39	-0.87
θ[deg]	+0.08	+2.32	-2.05
ψ[deg]	+1.35	+2.17	+0.49

IV. CONCLUSIONS AND FUTURE WORK

6-DoF EKF SLAM with global planar features in artificial environments was proposed. By measuring the position of planar landmarks, 6-Dof robot pose and the position of associated global planes are updated. The experiment showed that the proposed method had less accumulative error of estimation than comparative approaches.

Since bundle adjustment is not implemented although the proposed method merges landmarks when the revisits known places, the future work of this paper is developing a method to fix motion estimation drift by closing the loop. Another future work is applying the proposed method to outdoor environments. Outdoor ground is not complete plane. Therefore the method often does false matching so far.

REFERENCES

[1] M. A. Quddus, W. Y. Ochieng, and R. B. Noland, Current map-matching algorithms for transport applications: State-of-the art and future research directions, Transportation Research Part C: Emerging Technologies, Vol.15, No.5, pp.312–328, 2007.

[2] P. Skrzypczynski, Simultaneous localization and mapping: A feature-based probabilistic approach, International Journal of Applied Mathematics and Computer Science, Vol.19, No.4, pp.575–588, 2009.

[3] S. Thrun, W. Burgard and D. Fox, probabilistic robotics, The MIT Press, pp.309–336, 2005.

[4] S. Rusinkiewicz and M. Levoy, Efficient Variants of the ICP Algorithm, Proceedings Third International Conference on 3-D Digital Imaging and Modeling, pp.145–152, 2001.

[5] P. Biber and W. Straßer, The Normal Distributions Transform: A New Approach to Laser Scan Matching, Proceedings of the IEEE International Conference on Intelligent Robots and Systems, Vol.3, pp.2743–2748, 2003.

[6] M. Magnusson, A. Lilienthal and T. Duckett, Scan registration for autonomous mining vehicles using 3D‐NDT, Journal of Field Robotics, Vol.24, No.10, pp.803–827, 2007.

[7] J. Zhang and S. Singh, LOAM: Lidar Odometry and Mapping in Real-time, in Robotics: Science and Systems Conference, pp.161–195, 2014.

[8] Y. Taguchi, YD. Jian, S. Ramalingam and C. Feng, Point-Plane SLAM for Hand-Held 3D Sensors, Proceedings of IEEE International Conference on Robotics and Automation (ICRA), pp.5182–5189, 2013.

[9] S. Huang and G. Dissanayake, Convergence and Consistency Analysis for Extended Kalman Filter Based SLAM, IEEE Transactions on Robotics, Vol.23, No.5, pp.1036–1049, 2007.

[10] J. Martinez-Carranza and A. Calway, Unifying Planar and Point Mapping in Monocular SLAM, Proceedings of the British Machine Vision Conference (BMVC), pp.43.1–43.11, 2010.

[11] A. P. Gee, D. Chekhlov, WW. Mayol-Cuevas, A. Calway, Discovering Planes and Collapsing the State Space in Visual SLAM, Proceedings of British Machine Vision Conference, pp.1–10, 2007.

[12] A. P. Gee, D. Chekhlov, A. Calway, W. Mayol-Cuevas Discovering Higher Level Structure in Visual SLAM, IEEE Transactions on Robotics, Vol.24, No.5, pp.980–990, 2008.

[13] P. Kim, B. Coltin and H. J. Kim, Linear RGB-D SLAM for Planar Environments, Proceedings of The European Conference on Computer Vision (ECCV), pp.333–348, 2018.

[14] K. Takeuchi, M. Hashimoto and K. Takahashi, Laser-Based-3D Mapping by Human Walking in an Indoor Environment, The Science And Engineering Review Of Doshisha University, Vol.53, No.2, pp.84–91, 2012 (in Japanese).

[15] M. Pauly, M. Gross and L.P. Kobbelt, Efficient simplification of point-sampled surfaces, Proceedings of the conference on Visualization, pp.163–170, 2002.

[16] J.L. Bentley, Multidimensional binary search trees used for associative searching, Communications of the ACM, Vol.18, No.9, pp.509–517, 1975.

[17] S. Shimizu and Y. Kuroda, High-speed registration of point clouds by using dominant planes, Proceedings of the 19th Robotics Symposia, pp.453–458, 2014 (in Japanese).

[18] B.K.P. Horn, Extended gaussian images, Procceding of the IEEE, Vol.72, No.12, pp.1671–1686, 1984.

[19] J. Borenstein and L. Feng, Gyrodometry: a new method for combining data from gyros and odometry in mobile robots, Proceedings of IEEE International Conference on Robotics and Automation, pp.423–428, 1996.